Monitoring the Evolution of the Properties of PA-6/EPM-g-MA Blends in a Twin-Screw Extruder

A. V. MACHADO [1], M. VAN DUIN [2], and J. A. COVAS [1]

[1] Department of Polymer Engineering University of Minho 4800 Guimarães, Portugal

[2] DSM Research

P.O. Box 18, 6160 MD Geleen, The Netherlands

Abstract

The evolution of the properties of PA-6/EPM-g-MA blends are investigated along a twin-screw extruder in terms of chemical conversion, morphology development, and rheology evolution. Despite the interfacial structure of the various blends with different composition being distinct, an important decrease of the MA content at the first kneading zone from 0.5 to approximately 0.1wt.%MA and only a slight decrease further downstream is generally observed. In all cases in-situ compatibilization reactions occur in the melting zone within a few seconds. The relative differences in morphology can be directly explained by differences in blend composition. Although the morphology development along the extruder of the various blends as monitored by electron microscopy seems to follow a pattern similar to that of chemical conversion, their viscoelastic response shows a more gradual evolution.

INTRODUCTION

The preparation of polymer blends with interesting properties requires the capacity of morphology control (1-3). Compatibility and interfacial adhesion can be improved by the addition of suitable block or graft copolymers that act as interfacial agents or by reactive blending. A fine and stable morphology can then be produced, with the interfacial thickness increasing as a result of the interpenetration of the two types of chains across the interface (1-5).

However, blend morphology is also dictated by the blending conditions, i.e., the operating conditions and geometry of the equipment used. Many studies have correlated blend

composition, extruder or mixer layout and processing conditions with the morphology and mechanical properties of various blends. Less frequently, screws have been drawn from the extruder or samples have been taken from the melt, followed by off-line analysis, in order to gain some insight into the evolution of the process with time (5-7). In fact, upon reactive blending chemistry, morphology and rheology mutually interact and are influenced by local temperatures, residence times, velocity fields, and stress levels. Apparently, the major morphology changes along the length of a twin-screw extruder occur upon melting, in the first kneading section (6,8). In this type of experiment, the sample collecting technique is very important, since the morphology must be preserved both
during (induce low shear rates) and after collection (avoid relaxation of both matrix and dispersed phase after cessation of shear).

Reactive blends of PA-6 (polyamide 6) and EPM (eth-ylene-propylene rubber) (PA-6/EPM/EPM-g-MA, 80/20 w/w) were prepared in a co-rotating intermeshing twinscrew extruder fitted with various sampling devices capable of removing very quickly relevant samples from the extruder (9).

It was shown that the MA (maleic anhydride) content of the modified rubber decreases strongly upon melting of the PA pellets and melt flow through the first set of staggered kneading blocks, i.e., the grafting reaction is very fast. Simultaneously, the morphology changes dramatically in this zone of the extruder, from mm to (sub) μm level. Further downstream changes both in chemical conversion and morphology are very small. Measuring the evolution of the linear viscoelastic response of the blend along the extruder also provides important data for probing the chemistry and morphology development (10). The dynamic viscosity and the storage modulus decrease significantly upon melting of the components and are sensitive to the effect of the EPM-g-MA content. The phenomenon of PA-6 degradation was detected from the rheological data and confirmed by gel permeation chromatography, and determines the global rheological evolution along the extruder.

This work pursues the above studies but now concentrating on the effect of blend composition on the chemistry evolution and morphology development. By varying the composition of the PA-6/EPM-g-MA blend, different ratios of reactive groups (MA and amine) will be present, and hence the interfacial structure of the blends will be distinct and this could alter the rate of MA conversion. In turn, the morphology that could be anticipated from differences in blend composition could be modified.

EXPERIMENTAL

Materials

PA-6 (Akulon $^{(8)}$K123 with $M_n = 13.000\ g/mol, M_w = 25.000\ g/mol, NH_2 = 55 meq/g$ and $COOH = 60\ meq/g$) and EPM-g-MA (Exxelor VA 1801: 0.49wt% MA) were supplied by DSM, the Netherlands and Exxon, Spain, respectively.

Four blends (denoted 1 to 4) containing 80/20,50/ 50, 20/80 and 10/90 (PA-6/EPM-g-MA, w/w), respectively, were prepared in order to vary the ratio of reactive groups (amine and MA).

Blend Preparation

The blends were prepared in a laboratory modular Leistritz LSM 30.34 intermeshing co-rotating twinscrew extruder under identical operating conditions (set uniform temperature of 230°C, feed rate of 6 kg/h and screws rotating at 200 rpm). Figure 1 shows both the operating conditions selected and the extruder layout. The screws contain three mixing sections comprising staggered kneading blocks that will induce progressively significant dispersive and distributive mixing. The first kneading block is coupled to a reverse
conveying element, this assemblage causing complete melting and a big increase in interfacial area, while the third mixing section ensures adequate sealing for an efficient venting. Three sampling devices were inserted between barrel segments at the locations also depicted in Fig. 1 (and denoted as A, B and C, respectively). Here, not only high pressures are developed, which facilitates the detour of material from the screws towards the devices [for details of both operation and experiment assessment see reference (9)], but the main changes in morphology/chemistry are expected to occur.

Each device yields ~ 2 g of sample within 2 to 3sec – onds. In order to avoid further reaction and/or morphological changes such as coalescence of the dispersed phase, each sample was immediately quenched in liquid nitrogen for subsequent characterization.

Material Characterization

The PA-6 blend samples collected from the extruder were analyzed following the methodology adopted previously (4,10).

Milled samples were hydrolyzed with refluxing 6 N hydrochloric acid during 6 hours. Thin films of the residues were prepared by compression molding and analyzed by FT-IR (a Perkin Elmer 1720 spectrometer was available). The residual MA content was quantified using the anhydride carbonyl absorption at 1785 cm^{-1} after IR calibration with a set of references. The MA conversion (in %) is defined as $[(\ MA_{original} - MA_{residual}\ )/\ MA_{original}\ ] \times 100$.
Given the fine morphology of the blends produced, Transmission Electron Microscopy, TEM (Philips CM200), was used for obtaining the corresponding

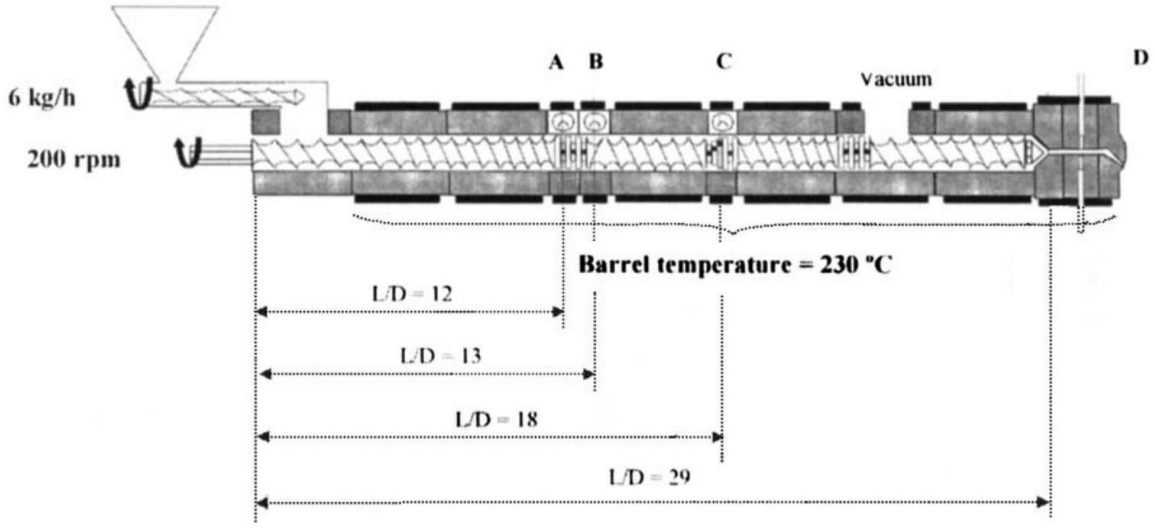

Fig. 1. Extruder layout and operating conditions. micrographs. Very thin slices of ~ 70 nm were cut at −100°C from samples previously stained with a 50/50 osmium tetroxide/formaldehyde mixture.

The rheological characterization was performed on a TA Instruments Weissenberg rheometer, using paral-lel-plate geometry (diameter = 40 mm) with a 2.00 mm gap. The nut-shaped samples collected from the extruder were compression molded for 10 minutes at 230°C under a pressure of 30 ton into discs 40 mm wide and 2 mm thick. Before any experiment, samples were vacuum dried at 80°C for 12 hours. Frequency sweeps (from 4×10^{-3} to 40 Hz) at 230°C were performed. A linearity check confirmed that strains up to 0.01 would keep the material's response in the linear viscoelastic domain. The nondestructive nature of small-amplitude oscillatory shear experiments for studying morphology/rheology correlations was also checked (10). Neither continuing low frequency deformation nor frequency sweeps of samples prepared with various compression times produced any noticeable changes in average particle diameters.

RESULTS AND DISCUSSION

Previous work (9) on the chemical conversion and morphology evolution of PA-6/EPM-g-MA blends (80/ 20w/w) along a similar twin-screw extruder revealed that an important chemical conversion (from 0.50 to 0.05wt%MA) and a significant decrease in particle size of the dispersed phase from a millimeter to a micrometer scale occurs upon melting in the first kneading block, given the rate of generation of interfacial area and the temperatures attained. In contrast, the above evolution is rather gentler downstream, despite the existence of further mixing sections. Only a decrease in particle size distribution seems to be observable. On the other hand, the amount of PA-6/EPM-gMA graft copolymer formed at the interface increases with increasing EPM-g-MA content (the MA content of the rubber phase was changed by varying the relative amount of EPM/EPM-g-MA), until a plateau is reached (9). The results presented in Fig. 2 showing the percentage of MA conversion along the extruder for the various blends are consistent with the above observations. Again, an important decrease of the MA content at the first kneading zone (location A) from 0.5 to approximately 0.1wt%MA and only a slight decrease further downstream is evident. For all the polyamide/ grafted rubber blends

(ranging from 80/20 to 10/90 w/w), the in-situ compatibilization reactions occur in the melting zone within a few seconds.

However, since the average length of the PA grafts decreases with the amount of PA-6, the interfacial structure in these blends must be distinct. For example, while in the case of blend 1(80/20, w/w) the original MA/amine molar ratio is 0.13 and PA chains are predominantly coupled to EPM-g-MA chains via the PA amine end groups, for blend 4 (10/90, w/w) the MA/ amine ratio is 4.5 but the MA conversion is still more or less complete. Thus, not only the PA amine end groups but also the PA chain amide groups must have reacted with EPM-g-MA, PA chain scission occurring, and resulting in relatively short lengths of the PA grafts. In addition, the water formed during the reaction between

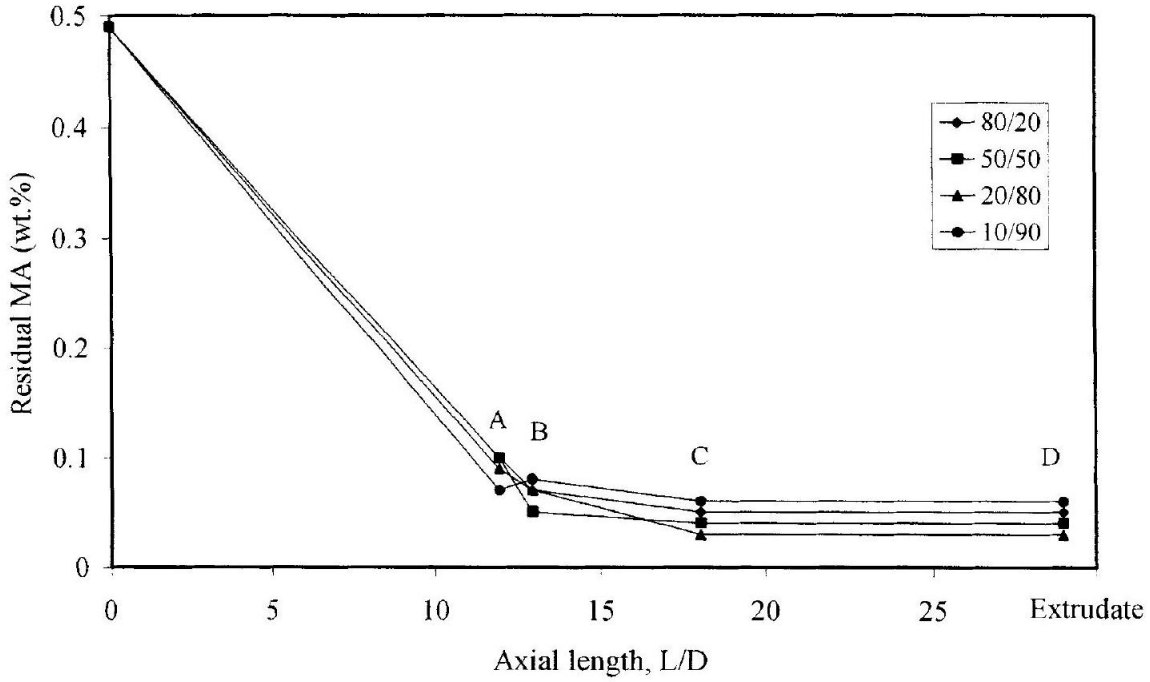

Fig. 2. MA conversion of the various blends along the screws and at the extruder outlet.
the PA amine end groups and the EPM-g-MA anhydride groups can hydrolyze the amide groups of the polyamide chain increasing chain scission (4). Direct degradation of the PA matrix can therefore be also anticipated.

The morphology development of the various blends along the extruder follows a pattern similar to that of chemical conversion. This can be concluded from Figs. 3 to 6, which reproduce TEM micrographs of blends 1 to 4, respectively.

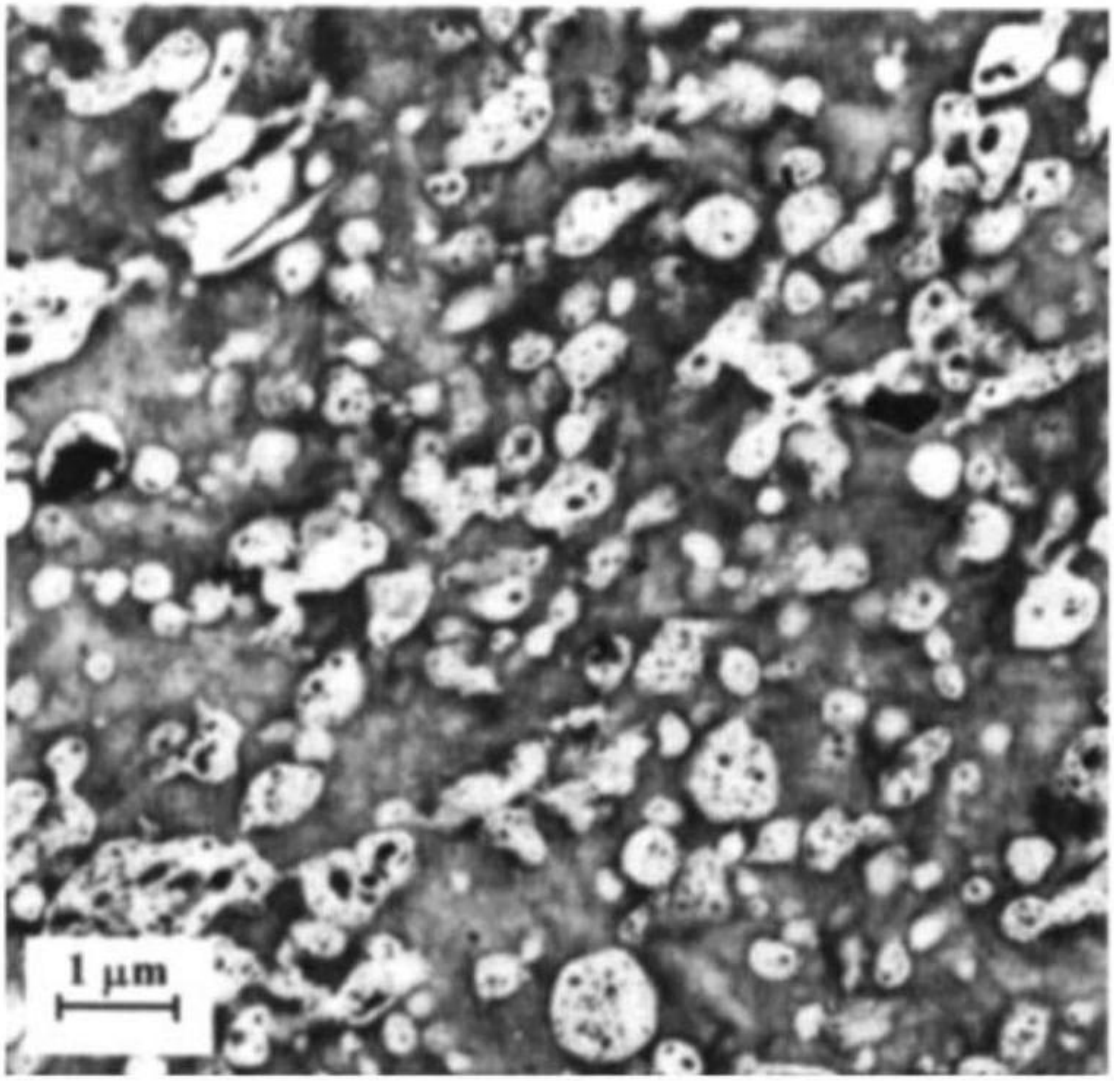

(a)

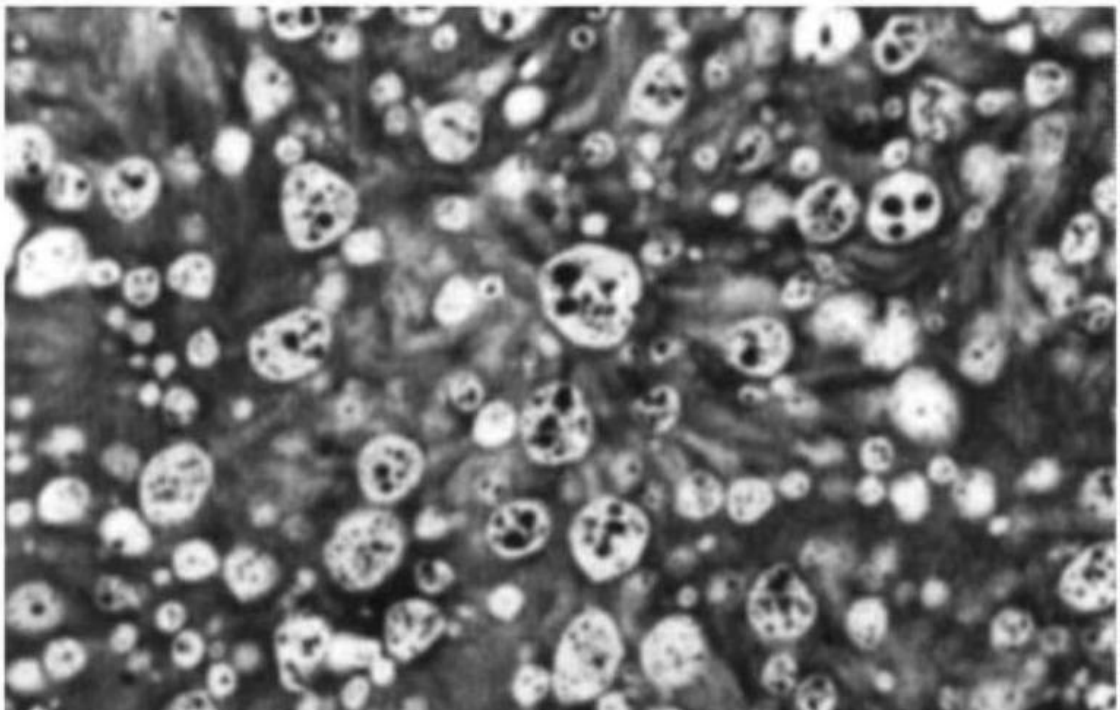

Figure 3 presents the morphology of blend 1 at locations A, B and C along the extruder (see Fig. 1) and at the die outlet, D. The matrix is PA-6, which has a melting temperature of 223°C. At location A (Fig. 3a) solid PA-6 coexists with melted material, an irregular morphology with both spherical and ribbon particles being visible. Previous studies (9,11) have indicated that initially the rubber becomes the continuous phase, surrounding the solid/smeared PA-6 pellets. Upon melting of the latter phase inversion should take place,

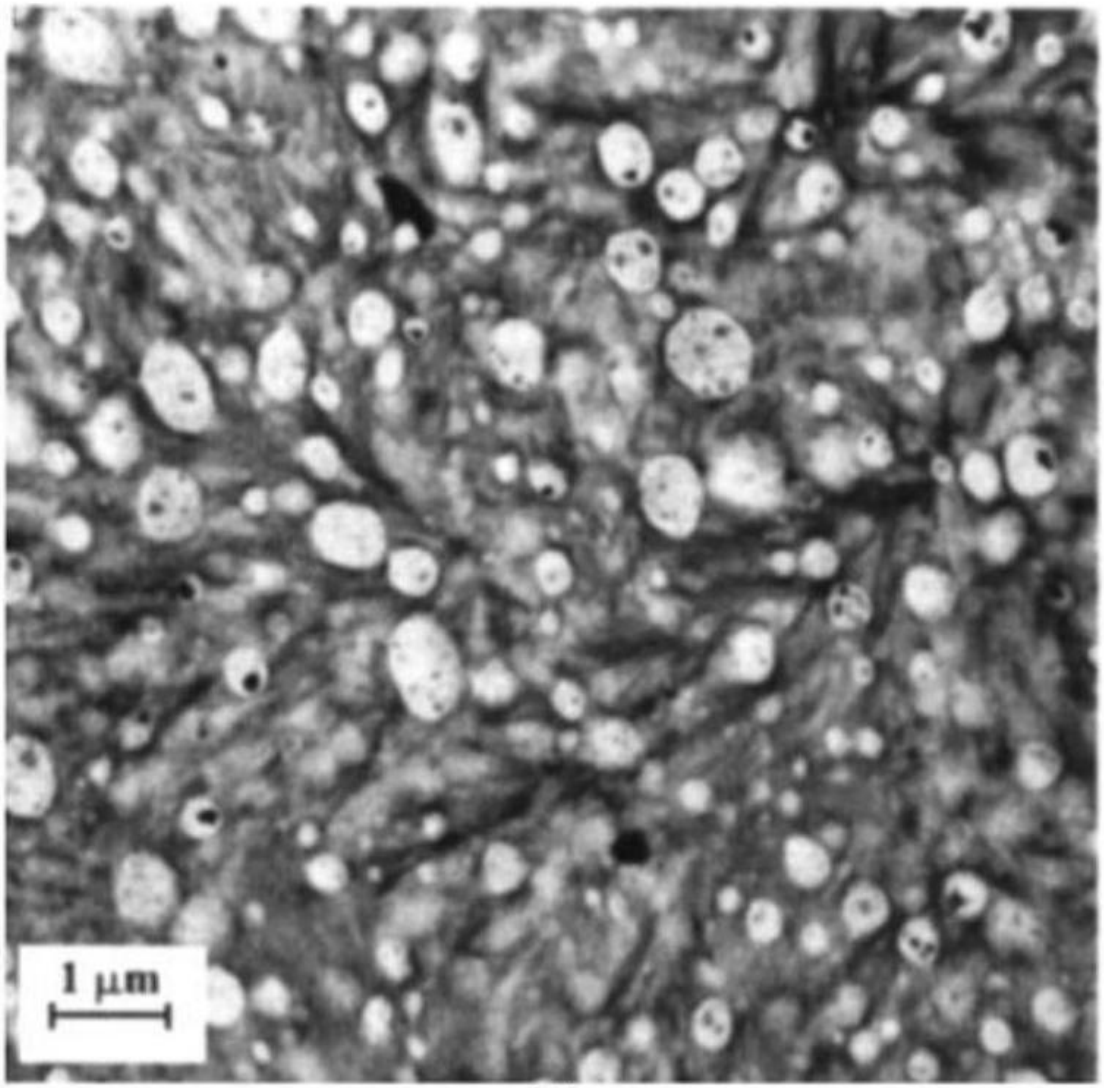

(c)

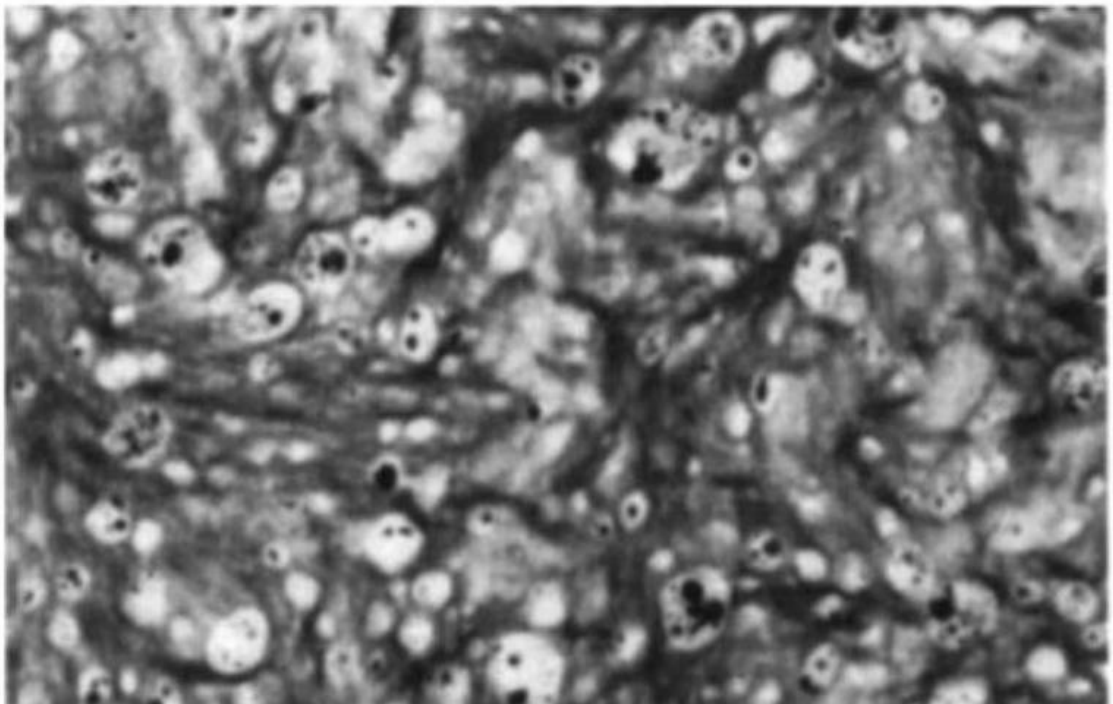

Fig. 3. Evolution of the morphology of blend 1 [PA-6/EPM-g-MA (80/20w/w)] along the screw axis; a) location A; b) location B; c) location C and d) extrudate.
i.e., rubber will constitute the dispersed phase. Although clear experimental evidence of this process is difficult to obtain, the occlusions present in the rubber particles support this hypothesis. As proposed by various authors (11-13), occlusions may be formed when the freshly molten PA-6 at the interface is drawn into the rubber phase while this becomes the dispersed phase. The degree of occlusion does not vary downstream along the extruder axis, which provides further support to the above reasoning. At location B (Fig. 3b), which is located 4 cm downstream of A, only fine regular spherical particles are present. A limited narrowing of the particle size distribution can be observed towards the die outlet (Figs. 3c and 3d).

In the case of blend 2(50/50w/w) the modified rubber is now the continuous phase, PA-6 elongated domains and small particles being observed. A bimodal dispersed phase consisting of $0.1 - 0.2\mu$ m and $1 - 7\mu$ m highly irregular particles can be identified both in locations A (Fig. 4a) and D (Fig. 4b), some coalescence appearing to have occurred in the latter. Unlike blend 1, here both components are already molten in location A; hence most of the MA groups have reacted (see Fig. 2), and further dispersion is not likely favorable.

Blend 3(20/80w/w) is a mirror of blend 1(80/20 w/w), thus it is interesting to compare the morphology evolution along the extruder axis for both cases (Figs. 3 and 5), Unlike blend 1 and similarly to blend 2, the morphology at location A shows a completely melted material with a good dispersion of the dispersed phase. While in blend 1 continuing mixing along the extruder would improve first the dispersion degree and then the dispersion homogeneity, blend 3 not only does not show any improvement downstream, but the formation of a few bigger particles seems to occur. Similar observations can be reported for blend 4, although fewer big particles seemed to be formed (Fig. 6).

The relative differences in morphology can be directly explained by differences in blend composition. As seen above, while in blend 1 (80/20, w/w) PA-6 is the matrix and the modified rubber the dispersed phase, in the remaining the opposite occurs. Also, at location A the former is only partially melted, while those richer in modified rubber are fully molten, which facilitates dispersion. In fact, the particles of the dispersed phase of blends 2-4 are generally much smaller and regular than those of blend 1 at location A. The presence of bigger PA-6 particles in the extrudate was unexpected and seems difficult to account for. As discussed above, with increasing modified rubber content the copolymer formed at the interface will contain shorter PA grafts. This could affect the interfacial thickness and consequently its strength, allowing for some coalescence to occur as the blend emerges from the die, since the material is still hot and no deformations are being imposed.

The rheological behavior of the various blends is determined from that of the individual components, their relative composition, degree of chemical conversion and existing morphology. Figures 7 and 8 show the variation of the storage, G' and loss moduli, G'' for both

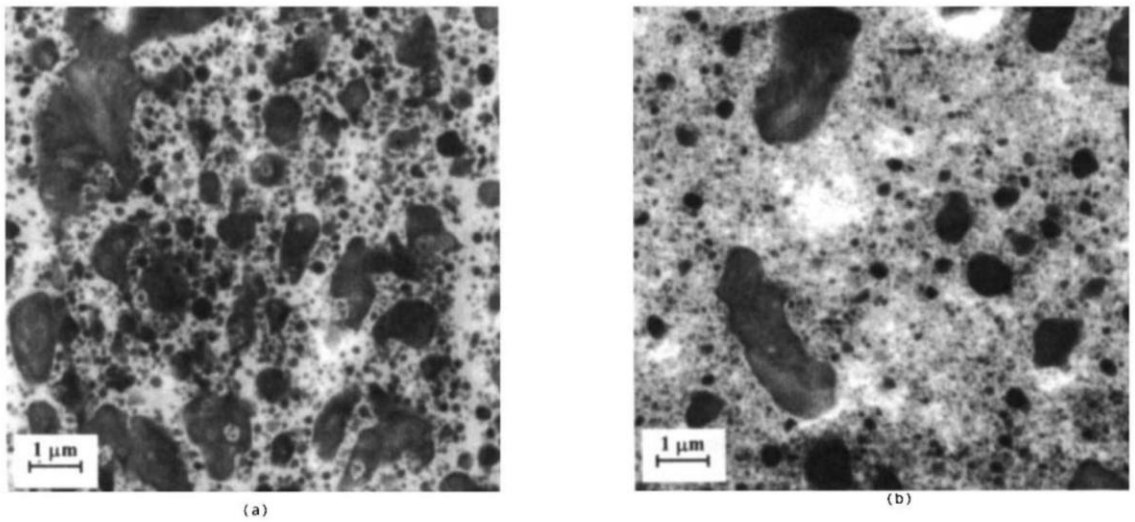

Fig. 4. Evolution of the morphology of blend 2 [PA-6/EPM-g-MA (50/50 w/w)] along the screw axis; a) location A; b) extrudate.

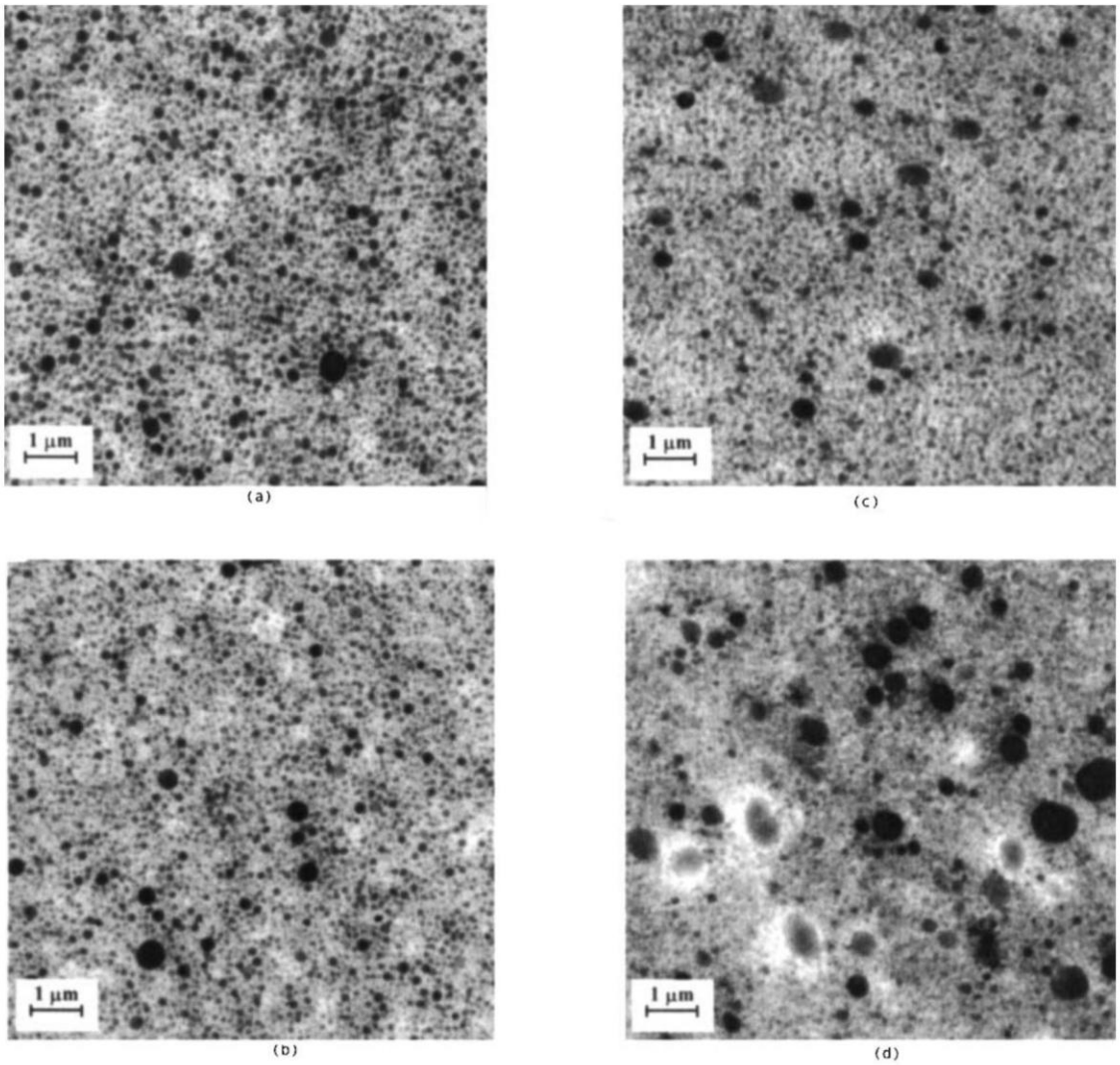

Fig. 5. Evolution of the morphology of blend 3 [PA-6/EPM-g-MA (20/80 w/w)] along the screw axis; a) location A; b) location B; c) location C and d) extrudate. the blends and the individual polymers at locations A (first kneading block) and D (extrudate), respectively.

Generally, these two rheological parameters are significantly higher for the blends than for their original components, owing to the development of a specific two-phase morphology and the formation of graft copolymer at the interface. The increase in elasticity at low frequencies is common with other systems (14,15) and is explained by the deformation and subsequent recovery of the dispersed phase particles due to interfacial tension and the rubbery nature of the EPM-g-MA phase. As reported previously (10), when PA-6 is processed alone under the same operating conditions used for the blends, progressive degradation due to chain scission takes place and both G' and G'' decrease. This is evident in both Figs. 7 and 8, by comparing the PA-6 curves at the A and D locations. As discussed above, in the case of blends PA-6 degradation can be even more

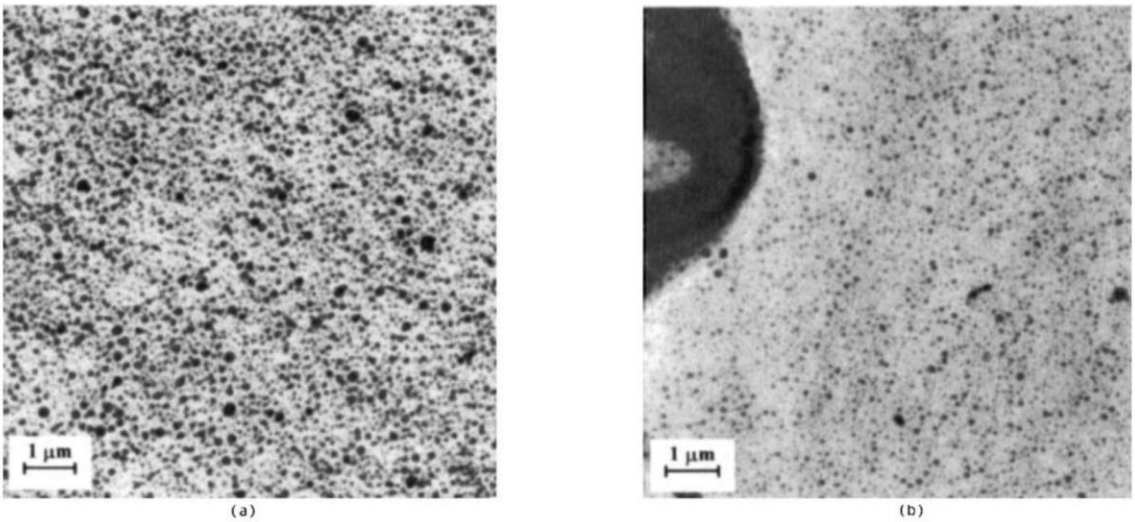

Fig. 6. Evolution of the morphology of blend 4 [PA-6/EPM-g-MA (10/90 w/w)] along the screw axis; a) location A; b) extrudate.

significant, as the water formed during the reaction between PA's amine end groups and EPM-g-MA's anhydride groups can hydrolyze the PA's amide groups increasing chain scission. Moreover, the EPM-g-MA's anhydride groups can also react with the PA amide chain groups, degrading PA.

The influence of blend composition can be easily identified in the lower frequency range. Both G' and G'' increase from blend 1 to blend 2 and decrease thereafter, but the values of blend 4 are always much higher than those of blend 1. This would be expected, since both the elasticity and the viscosity of EPM-g-MA are higher than those of PA-6. On the other hand, in blends rich in rubber the progressive decrease of G' and G'' with increasing rubber content should be due to the combined effects of average particle size of the PA-6 particles, amount and shape of the bigger particles and thickness of the interface. As proposed above, decreasing interface thickness will lower the adhesion between the two phases and consequently, both the blend elasticity and viscosity.

While monitoring the residual MA content and morphology changes along the screw did not yield any significant evolution in the blends characteristics from location A onwards, rheology measurements indicated coherent trends. With the exception of blend 1, which exhibits an important decrease in G' and G'' at low frequencies from location A to D that can be explained by the already discussed PA- 6 degradation, G' and (less significantly) G'' of the remaining blends increase towards the die, certainly because of an enhancement of the dispersion. However, this improvement decreases with increasing rubber content, which is consistent with the hypothesis of a progressively weaker interface.

CONCLUSIONS

Despite the frequent industrial production of new polymer blends by reactive extrusion, the understanding of the complex physico-chemical processes developing in the extruder are still not fully understood. The present work shows a correlation between morphology

and chemical conversion in the case of PA-6/EPM-g-MA blends with various compositions. Most of the chemical conversion and morphology evolution occurred within a few seconds over a few centimeters along the extruder axis, during melting of the components and regardless of the initial blend composition. Once the MA groups of EPM-g-MA are almost completely converted, the morphology becomes also fully developed. Rheological parameters seem to be able to discriminate very similar morphologies. Although graft copolymers formed at the interface provide steric stabilization and prevent coalescence, their efficiency seems to decrease at high modified rubber contents owing to shorter PA grafts.

ACKNOWLEDGMENTS

The authors are grateful to R. Tandler, at DSM, Geleen, the Netherlands, for obtaining most of the TEM micrographs, to DSM and to Exxon (Spain) for materials and to INVOTAN, Portugal, for financing the travel of one of the authors to Geleen.

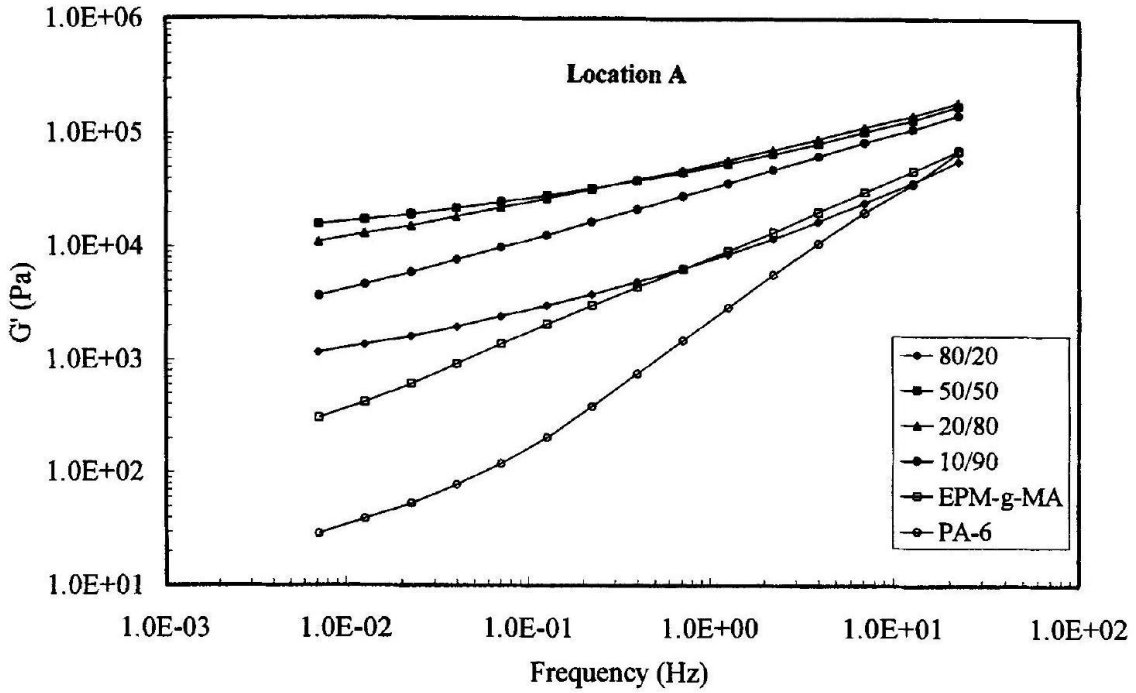

(a)

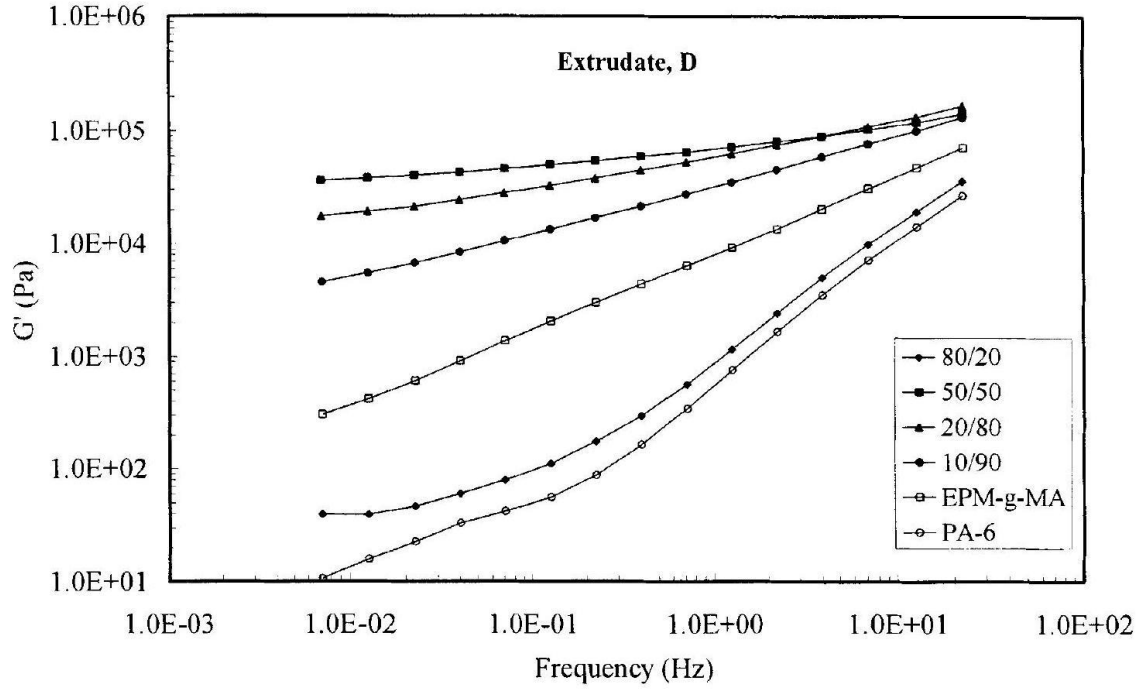

(b)

Fig. 7. Storage modulus, G', of both blends 1-4 and individual components (PA-6 and EPM-g-MA) at location A (a) and die outlet (b).

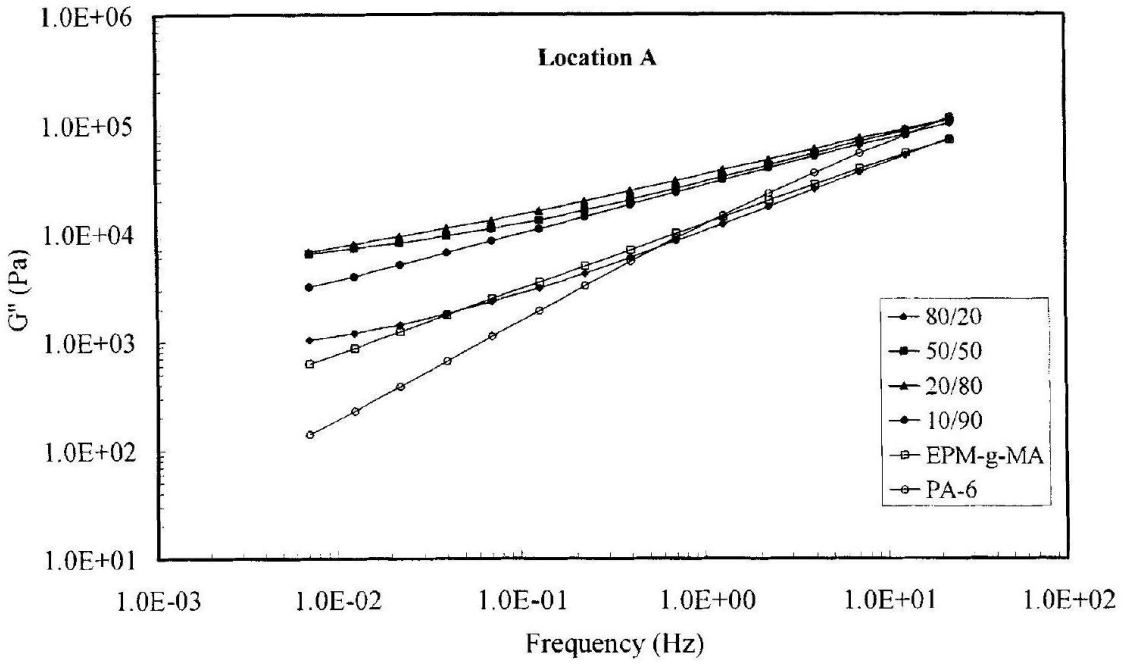

(a)

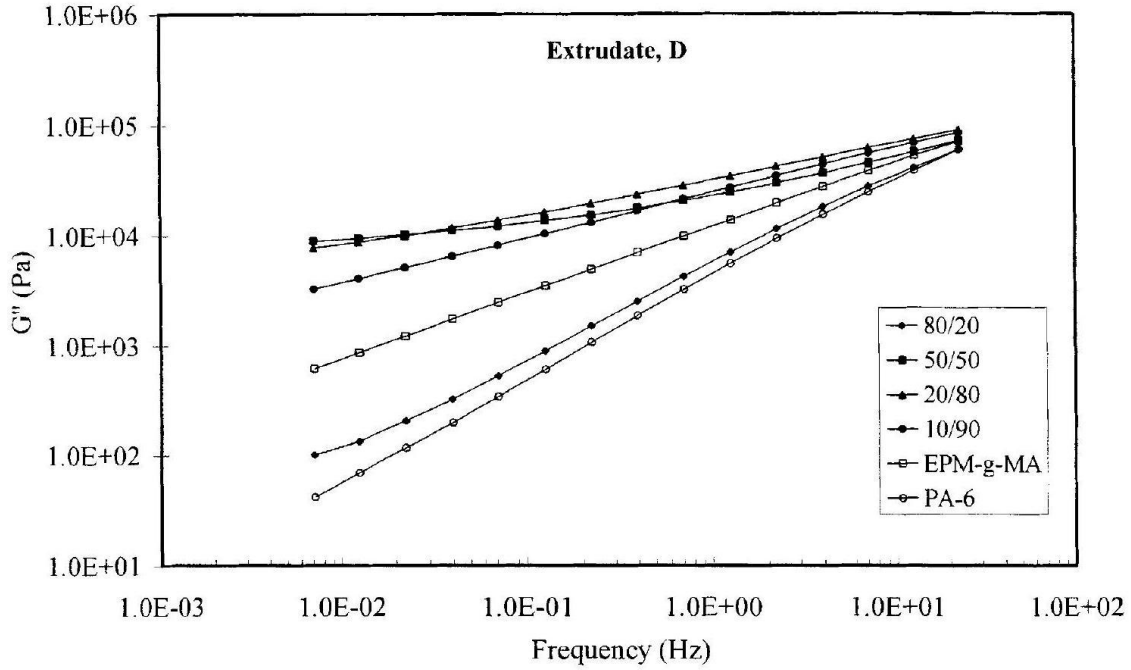

(b)

Fig. 8. Loss modulus, G'', of both blends 1-4 and individual components (PA-6 and EPM-g-MA) at location A (a) and die outlet (b).

REFERENCES

1. S. Datta and D. Lohse, Polymeric Compatibilizers, Hanser Publishers, New York (1996).
2. L. A. Utracki, Encyclopaedic Dictionary of Commercial Polymer Blends, ChemTec Publishing, Toronto (1994).
3. S. Datta and D. J. Lohse, Polymeric Compatibilizers, Uses and Benefits in Polymer Blends, Hanser Publishers, Munich (1996).
4. M. van Duin, M. Aussems, and R. J. M. Borggreve, J. Polym. Sci: Part A: Polym. Chem., 36, 179 (1998).
5. H. Cartier and G. H. Hu, J. Polym. Eng. Sci, 39, 996 (1999).
6. M. Stephan, O. Franzheim, T. Rische, P. Heidemeyer, U. Burkhardt, and A. Kiani, Adv. Polym. Tech., 16, 1 (1997).
7. T. Sakai, Adv. Polym. Tech., 14, 277 (1995).
8. U. Sundararaj and C. W. Macosko, Polym. Eng. Sci., 36, 1769 (1996).
9. A. V, Machado, J. A. Covas, and M. van Duin, J. Polym. Sci: Part A: Polym. Chem., 37, 1311 (1999).
10. J. A. Covas, A. V. Machado, and M. van Duin, Adv. Polym. Tech., 19, 260 (2000).
11. A. V. Machado, J. A. Covas, and M. van Duin, J. Appl. Polym. Sci., 80, 1535 (2001).
12. U. Sundararaj and C. W. Macosko, Polym. Eng. Sci., 38, 1769 (1996).
13. C. E. Scott and C. W. Macosko, Polym. Bulletin, 26, 341 (1991).
14. M. Bousmina and R. Muller, Rheol. Acta, 35, 369 (1996).
15. C. Lacroix, M. Aressy, and P. J. Carreau, Rheol. Acta, 36, 416 (1997).